

**Synchronization of networked chaotic oscillators under external periodic driving**Wenchao Yang,<sup>1,\*</sup> Weijie Lin,<sup>2,3</sup> Xingang Wang,<sup>2,†</sup> and Liang Huang<sup>1,‡</sup><sup>1</sup>*Institute of Computational Physics and Complex Systems and Key Laboratory for Magnetism and Magnetic Materials of MOE, Lanzhou University, Lanzhou, Gansu 730000, China*<sup>2</sup>*School of Physics and Information Technology, Shaanxi Normal University, Xi'an 710062, China*<sup>3</sup>*Department of Physics, Zhejiang University, Hangzhou 310027, China*

(Received 25 November 2014; published 19 March 2015)

The dynamical responses of a complex system to external perturbations are of both fundamental interest and practical significance. Here, by the model of networked chaotic oscillators, we investigate how the synchronization behavior of a complex network is influenced by an externally added periodic driving. Interestingly, it is found that by a slight change of the properties of the external driving, e.g., the frequency or phase lag between its intrinsic oscillation and external driving, the network synchronizability could be significantly modified. We demonstrate this phenomenon by different network models and, based on the method of master stability function, give an analysis on the underlying mechanisms. Our studies highlight the importance of external perturbations on the collective behaviors of complex networks, and also provide an alternate approach for controlling network synchronization.

DOI: [10.1103/PhysRevE.91.032912](https://doi.org/10.1103/PhysRevE.91.032912)

PACS number(s): 05.45.Xt, 89.75.Hc

**I. INTRODUCTION**

Realistic systems are inevitably disturbed by external perturbations, from either the surrounding environments or some specially designed controllers, and one of the central tasks in nonlinear science has been exploring the responses of complex dynamical systems to various perturbation signals [1,2]. In biological and engineering systems, it is commonly recognized that many of the system functions rely heavily on the externally added periodic signals, examples of which include the entrainment of the rhythm of suprachiasmatic nucleus (SCN) to the 24-h daily light-dark cycle [3], the synchronization of different brain regions to the SCN rhythm [4], and the regulation of the heart beating rate to the rhythm of the sinoatrial node (SAN) [5], the coordination of a large of remote sensors or computing units by the timing signals of the global positioning system (GPS) [6], etc. To properly understand the functioning of these systems, in the past decades there have been continuous efforts in studying the responses of complex dynamical systems to externally added periodic forces. For instance, mimicking the light-dark cycle by an external periodic driving, it has been shown that an ensemble of phase oscillators coupled through different network structures can be successfully entrained to the same frequency [7,8]; replacing the SAN signals by a linearly or circularly polarized electric field, it has been demonstrated that the spatiotemporal irregularity underlying life-threatening cardiac arrhythmias, e.g., fibrillation and spiral waves, can be efficiently eliminated, therefore recovering the coherent beating of the heart cells [9,10]; using sinusoidal waves as the information signals, it has been shown that the signals can be properly detected and transmitted on networks of coupled nonlinear oscillators [11,12].

A typical phenomenon observed in systems of coupled oscillators is synchronization, which has been widely regarded as the dynamical basis for many of the system functions [13]. Generally speaking, synchronization refers to the coherent motion of coupled oscillators, which usually occurs when the coupling strength between the oscillators exceeds some threshold values. Depending on the specific form of the coherent motion, different types of synchronization have been observed and studied in the past, including complete synchronization, phase synchronization, generalized synchronization, etc. [13,14]. Recently, stimulated by the discoveries of the small-world and scale-free features in many natural and manmade systems [15,16], a new surge of research interest has been appeared in studying the synchronization of complex networks, where the important roles of network structure on synchronization have been revealed and addressed [17–22]. In studying network synchronization, a prevalent method is the master stability function (MSF), which suggests that the synchronizability of a complex network is largely determined by an eigenratio calculated from the eigenvalues of the network coupling matrix [23–26]. Specifically, the smaller the eigenratio is, the higher the propensity for a network to be synchronized. Regarding this, to enhance the synchronizability of a complex network, the central task seems to be only finding methods for decreasing the eigenratio, by either adjusting the network topology or adopting new coupling schemes [17–21].

While the importance of network structure and coupling scheme on synchronization has been well addressed, little attention has been paid to the possible influences of external perturbations on network synchronization. According to MSF, whether a network can be synchronized is jointly determined by two factors: the distribution of the eigenvalues and the shape of the MSF curve. The latter, which defines the stable region for synchronization, is determined by only the low-dimensional node dynamics. If by some methods, e.g., driving the oscillators by some externally added perturbations, the MSF curve could be modified in such a way that the synchronization region is greatly enlarged, then it will be possible to modify the network synchronizability

\*Present address: Department of Radiology, Medical Physics, University Medical Center Freiburg, Freiburg 79106, Germany.

†wangxg@snnu.edu.cn

‡huangl@lzu.edu.cn

without changing the network structure and coupling scheme. Inspired by this, in this article we study the synchronization of networked chaotic oscillators when an externally added periodic driving is presented. Interestingly, we find that by a slight change of the frequency or the phase lag of the driving signals, the synchronization behaviors of complex networks can be significantly modified. This finding gives insights on the functioning of some biological systems where an external periodic driving is presented, e.g., the SCN and SAN, and also provides an efficient approach for controlling the synchronization behaviors of complex networks. In Sec. II, we shall present the network model, and demonstrate the sensitive dependence of the network synchronization on the frequency of the external driving. In Sec. III, based on the MSF method, we shall give an analysis on the underlying mechanism for the observed phenomenon. In Sec. IV, we shall generalize our studies to other network models, and discussing the effect of phase lag of the driving on network synchronization. Finally, in Sec. V we shall give our discussions and conclusion.

## II. MODEL AND PHENOMENON

Our model of networked chaotic oscillators with external periodic driving reads [8,21]

$$\dot{\mathbf{x}}_i = \mathbf{F}(\mathbf{x}_i) - \varepsilon \sum_{j=1}^N c_{ij} [\mathbf{H}(\mathbf{x}_j) - \mathbf{H}(\mathbf{x}_i)] + \mathbf{g}(t), \quad (1)$$

with  $i, j = 1, \dots, N$  the oscillator (node) indices and  $\mathbf{x}$  the state variables. In the isolated form, the dynamics of each oscillator is governed by the equation  $\dot{\mathbf{x}}_i = \mathbf{F}(\mathbf{x}_i)$ , which, for the sake of simplicity, is set as identical over the network.  $\mathbf{H}(\mathbf{x})$  denotes the coupling function and  $\varepsilon$  is the uniform coupling strength. The coupling relationship of the oscillators is described by the coupling matrix  $\mathbf{C}$ , with  $c_{ij} = -a_{ij}/k_i$  and  $c_{ii} = 1$ . Here,  $\mathbf{A}$  is the adjacency matrix constructed as follows:  $a_{ij} = 1$  if nodes  $i$  and  $j$  are directly connected in the network; otherwise,  $a_{ij} = 0$ .  $k_i = \sum_j a_{ij}$  counts for the number of connections for node  $i$ , i.e., the node degree. All oscillators are subjected to the same periodic driving  $\mathbf{g}(t) = \mathbf{b} \sin(\omega t + \phi_0)$ , with  $\mathbf{b}$ ,  $\omega$ , and  $\phi_0$  the amplitude, frequency, and phase lag of the driving, respectively. Note that here we assume the normalized coupling. But since our results are mostly based on the MSF approach, where the effects of different network topology and coupling schemes (normalized, weighted, unweighted, etc.) are solely determined by their spectra of eigenvalues, therefore, our results should be able to apply to other types of network and linear coupling schemes straightforwardly. Another point that needs clarifying is the coupling function  $\mathbf{H}(\mathbf{x})$ . Here we assume linear coupling without delay. However, a more general coupling function would be a pairwise function of the form  $\mathbf{H}(\mathbf{x}_i, \mathbf{x}_j)$ , which could be nonlinear and including delay. For nonlinear coupling, it may introduce peculiar unsynchronized phenomena due to the nonlinear interactions. However, around the synchronization manifold, the difference between  $\mathbf{x}_i$  and  $\mathbf{x}_j$  is small; thus the coupling will be dominated by the linear term  $\mathbf{x}_j - \mathbf{x}_i$ . Since  $\mathbf{x}_i$  can be absorbed into the node dynamics  $\mathbf{F}(\mathbf{x}_i)$ , the coupling can then be written as  $\mathbf{H}(\mathbf{x}_j)$ , as adopted in Eq. (1). Therefore, for nonlinear coupling with the linear term as the lowest order of approximation, the synchronization behavior

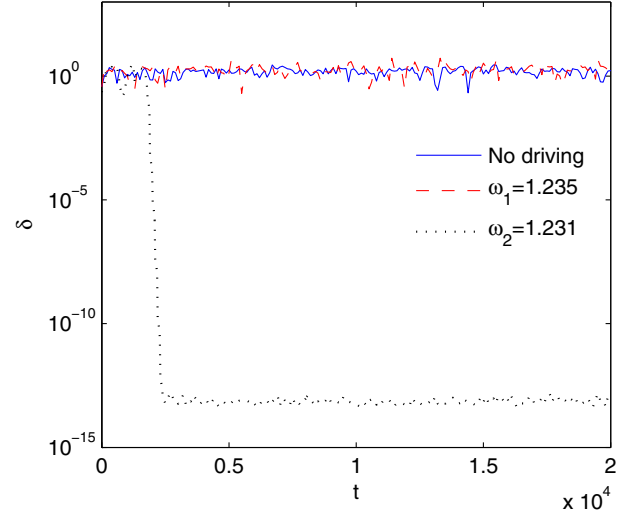


FIG. 1. (Color online) For an ER network of  $N = 100$  chaotic Rössler oscillators and average degree  $\langle k \rangle = 10$ , by the coupling strength  $\varepsilon = 0.9$ , the time evolutions of the network synchronization error,  $\delta$ , for the cases of no external driving (solid line), and external driving with amplitude  $b = 4$  but different frequencies:  $\omega_1 = 1.235$  (dashed line) and  $\omega_2 = 1.231$  (dotted line). The relevant eigenvalues for the coupling matrix are  $\lambda_2 = 0.180$  and  $\lambda_N = 1.783$ . All the following simulations of synchronization dynamics are carried out on the same ER random network.

will be similar to the results presented in this paper, although the unsynchronous dynamics could be totally different. For the case with delay in the coupling, the synchronization dynamics can be very different due to the new dimension of delay [27]. Our results could not be applied to that case, and it deserves future investigation.

We start by demonstrating the sensitive dependence of the network synchronization on the frequency of the external driving. Our first model is a random network of  $N = 100$  coupled chaotic Rössler oscillators. The network is generated by the Erdős-Renyi (ER) model, with the average degree  $\langle k \rangle = 10$ . The Rössler oscillator in its isolated form is described by the equations  $(dx/dt, dy/dt, dz/dt)^T = (-y - z, x + \alpha y, \beta + xz - \gamma z)^T$ . We set the parameters  $(\alpha, \beta, \gamma) = (0.2, 0.2, 9)$ , with which the oscillator presents chaotic dynamics [28]. The oscillators are coupled through the  $x$  variable, i.e.,  $\mathbf{H}([x, y, z]^T) = [x, 0, 0]^T$ . The external driving is added on the  $x$  variable of each oscillator too, i.e.,  $(b_x, b_y, b_z) = (b, 0, 0)$ . We measure the degree of network synchronization by the error  $\delta = \sum_i |x_i - \langle x \rangle| / N$ , with  $\langle x \rangle$  averaged over all the oscillators. Clearly, the smaller  $\delta$  is, the better the network synchronization will be. In our studies, we fix the coupling strength as  $\varepsilon = 0.9$ , with which the network is staying in the nonsynchronous state when the external driving is absent (Fig. 1). We now drive the oscillators by a periodic driving of amplitude  $b = 4$  and phase lag  $\phi_0 = 0$ . Within the range  $[0, 3]$ , we randomly select a frequency  $\omega_1 = 1.235$ , and plot in Fig. 1 the time evolution of  $\delta$ . It is seen that, comparing to the undriven case, the network synchronization is not improved at all. By another randomly selected frequency  $\omega_2 = 1.231$ , we monitor the network evolution again. Surprisingly, it is

found that the synchronization error quickly decreased to zero. That is, by a slight change of the driving frequency ( $\Delta\omega = 4 \times 10^{-3}$ ), the network changed abruptly from the nonsynchronous to synchronous state.

The above phenomenon of frequency-sensitive network synchronization is commonly observed in our simulations, despite the changes of the driving amplitude and the phase lag. As we will show later, this phenomenon is also observable for other types of node dynamics. The numerical evidences therefore imply the universality of this phenomenon in systems of networked oscillators, making it interesting to explore the underlying mechanism.

### III. MECHANISM ANALYSIS

We next analyze the influence of the driving frequency on network synchronizability, based on the MSF method [23,24]. Let  $\mathbf{x}_s$  be the trajectory that all the oscillators are synchronized to, i.e., the synchronous manifold, and  $\delta\mathbf{x}_i = \mathbf{x}_i - \mathbf{x}_s$  be the infinitesimal perturbations added to the trajectory of the  $i$ th oscillator; then in the linearized form the perturbations will be evolving according to the following variational equation:

$$\delta\dot{\mathbf{x}}_i = \mathbf{D}\mathbf{F}(\mathbf{x}_s) - \varepsilon \sum_{j=1}^N c_{ij} \mathbf{D}\mathbf{H}(\mathbf{x}_s)(\delta\mathbf{x}_j - \delta\mathbf{x}_i), \quad (2)$$

with  $\mathbf{D}\mathbf{F}$  and  $\mathbf{D}\mathbf{H}$  the Jacobian matrices of the corresponding vector functions evaluated on  $\mathbf{x}_s$ . Projecting  $\{\delta\mathbf{x}_i\}$  into the eigenspace spanned by the eigenvectors of the Laplacian coupling matrix  $\mathbf{G} = \mathbf{C} + \mathbf{I}$  ( $\mathbf{I}$  is the identity matrix of the same dimension as  $\mathbf{C}$ ), then the set of equations described by Eq. (2) can be transformed into  $N$  blocked variational equations of the form

$$\delta\dot{\mathbf{y}}_i = [\mathbf{D}\mathbf{F}(\mathbf{x}_s) - \varepsilon\lambda_i \mathbf{D}\mathbf{H}(\mathbf{x}_s)]\delta\mathbf{y}_i, \quad (3)$$

with  $0 = \lambda_1 < \lambda_2 \leq \dots \leq \lambda_N$  the eigenvalues of  $\mathbf{G}$ , and  $\delta\mathbf{y}_i$  the  $i$ th mode of the perturbations. Denoting  $\Lambda_i$  as the largest Lyapunov exponent calculated from Eq. (3) for the  $i$ th mode, then the stability of this mode is determined by the sign of  $\Lambda_i$ : the mode  $i$  is stable if  $\Lambda_i \leq 0$  ( $\delta\mathbf{y}_i$  approaches zero as time increases), and is unstable if  $\Lambda_i > 0$ . It is worth noting that the mode of  $\lambda_1$  represents the motion parallel to the synchronous manifold, which for the driving-free case has the same dynamics as the isolated chaotic oscillator, but may follow different dynamics when the external driving is present.

To achieve the network synchronization, a necessary condition is that all the nontrivial eigenmodes are stable, i.e.,  $\Lambda_i < 0$  for  $i = 2, \dots, N$ . Defining  $\sigma \equiv \varepsilon\lambda$ , then the analysis of network synchronization can be decoupled into two separate issues: the variation of  $\Lambda$  as a function of  $\sigma$  [i.e., the MSF curve calculated from Eq. (3)] and the distribution of the eigenvalues (calculated from the Laplacian coupling matrix  $\mathbf{G}$ ). For the typical chaotic oscillators and coupling functions,  $\Lambda$  is negative only within a bounded region in the parameter space, saying  $\sigma \in (\sigma_1, \sigma_2)$ . As network synchronization requires  $\varepsilon\lambda_2 > \sigma_1$  and  $\varepsilon\lambda_N < \sigma_2$ , the propensity of network synchronization thus can be characterized by the eigenratio  $R \equiv \lambda_N/\lambda_2$ . Specifically, given  $R < R_c = \sigma_2/\sigma_1$ , network synchronization in principle can be reached by adjusting the coupling strength. In this regard, the smaller  $R$  is, the higher

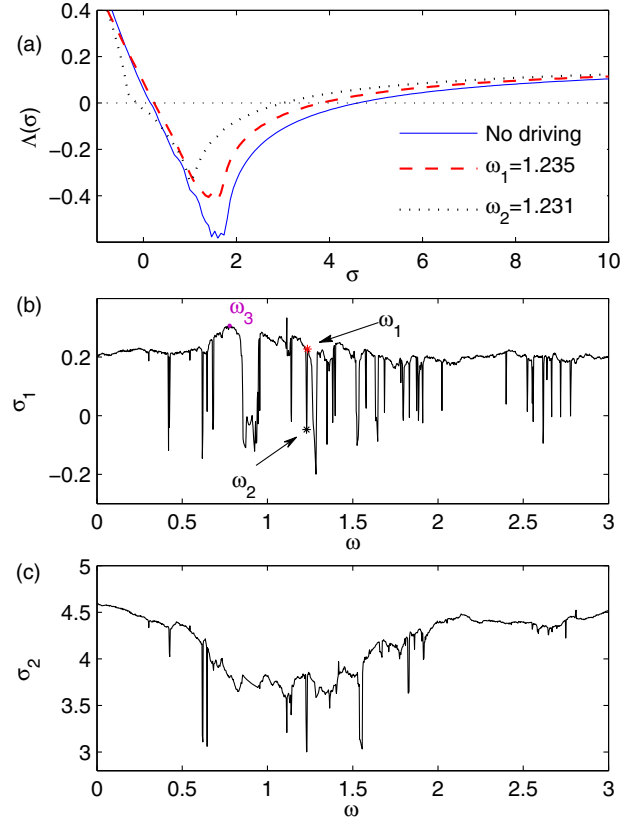


FIG. 2. (Color online) For the same network model used in Fig. 1, the influence of the driving frequency on the MSF curve. (a) The MSF curves for the cases of no external driving (solid line), and external driving with amplitude  $b = 4$  but for different frequencies:  $\omega_1 = 1.235$  (dashed line) and  $\omega_2 = 1.231$  (dotted line). (b)  $\sigma_1$  vs  $\omega$ . (c)  $\sigma_2$  vs  $\omega$ .  $\sigma_1$  and  $\sigma_2$  denote, respectively, the left and right boundaries of the stable region.

the network synchronizability usually is [25]. This criterion has led a number of studies on the optimization of network synchronization, by either modifying the network structure or changing the coupling scheme of the oscillators [18–22,29,30].

By the MSF method described above, we now give an analysis on the phenomenon observed in Fig. 1. When the external driving is absent, the synchronous manifold has the same dynamics as the isolated chaotic oscillator,  $\dot{\mathbf{x}}_s = \mathbf{F}(\mathbf{x}_s)$ . By numerically solving Eq. (3), we plot in Fig. 2(a) the variation of  $\Lambda$  with  $\sigma$ , i.e., the MSF curve. It is seen that  $\Lambda$  is negative in the bounded region  $\sigma \in (0.186, 4.614)$ . For the generated network structure of an ER network of  $N = 100$  and  $\langle k \rangle = 10$ , we have  $\lambda_2 = 0.180$  and  $\lambda_N = 1.783$ . As  $\varepsilon\lambda_2 = 0.162 < \sigma_1$ , the network therefore is judged as nonsynchronizable according to the MSF analysis. This is in agreement with the numerical result shown in Fig. 1. When external driving is presented, the synchronous manifold is governed by the equation

$$\dot{\mathbf{x}}_s = \mathbf{F}(\mathbf{x}_s) + \mathbf{g}(t). \quad (4)$$

Setting the driving amplitude as  $b = 4$ , we plot in Fig. 2(a) again the MSF curve. It is seen that for the frequency  $\omega_1 = 1.235$ , the boundaries of the stable region are only slightly adjusted, and the mode of  $\lambda_2$  is still staying in the

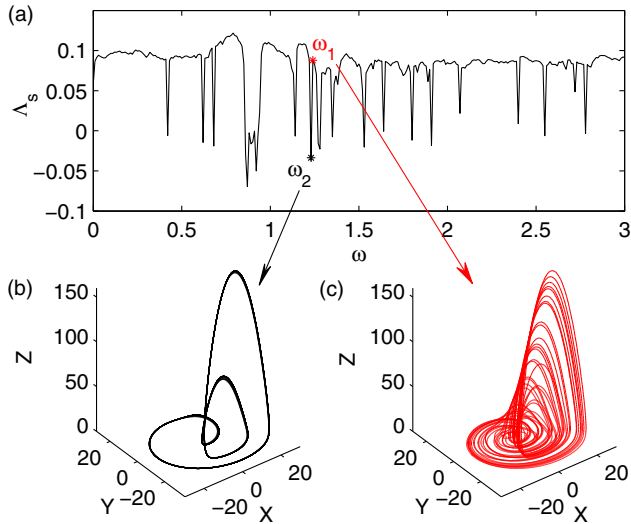


FIG. 3. (Color online) (a) For  $b = 4$ , the variation of the largest Lyapunov exponent of the synchronous manifold,  $\Lambda_s$ , as a function of the driving frequency,  $\omega$ , calculated according to Eq. (4). (b) The periodic motion at  $\omega_2 = 1.231$ , with  $\Lambda_s = -0.0367$ . (c) The chaotic motion at  $\omega_1 = 1.235$ , with  $\Lambda_s = 0.088$ .

unstable region. However, for the frequency  $\omega_2 = 1.231$ , it is seen that the boundaries of the stable region are significantly modified. To be more specific, the left and right boundaries of the stable region are adjusted to  $\sigma_1 = -0.047$  and  $\sigma_2 = 2.994$ , respectively. As now all modes are staying inside the stable region, the network thus becomes synchronizable.

To have a global picture on the influence of the driving frequency on the MSF curve, we plot in Figs. 2(b) and 2(c) the variation of the boundaries of the stable region,  $\sigma_1$  and  $\sigma_2$ , as a function of  $\omega$ . It is seen that as  $\omega$  increases from zero to 3, both  $\sigma_1$  and  $\sigma_2$  vary wildly with large amplitudes. Particularly, at some frequencies it is observed that  $\sigma_1$  ( $\sigma_2$ ) is suddenly dropped to very small or even negative values, e.g.,  $\sigma_1 = -0.047$  at  $\omega_2 = 1.231$ , while at some frequencies  $\sigma_1$  ( $\sigma_2$ ) is larger than that of the driving-free case, e.g.,  $\sigma_1 = 0.307$  at  $\omega_3 = 0.781$ .

According to Eq. (3), for the given coupling function, the MSF curve is solely determined by the synchronous manifold  $\mathbf{x}_s$ . To explore the nature of the modified MSF curve, we next study the dependence of the node dynamics on the driving frequency. In Fig. 3(a), we plot the largest Lyapunov exponent of the synchronous manifold,  $\Lambda_s$ , as a function of  $\omega$ . [Please note that  $\Lambda_s$  is calculated according to Eq. (4), instead of Eq. (3) by setting  $\varepsilon = 0$ .] It is seen in this figure that, similar to the behavior of  $\sigma_{1,2}$  [Fig. 2(a)],  $\Lambda_s$  also varies wildly with  $\omega$ . A careful checking with the variations of  $\sigma_1$  and  $\Lambda_s$  also shows that they are varying with the same steps. In particular, for the frequencies  $\omega_1 = 1.235$  and  $\omega_2 = 1.231$  used in Fig. 1, we have  $\Lambda_s = 0.088$  and  $-0.0367$ , respectively. As negative (positive)  $\Lambda_s$  characterizes periodic (chaotic) motion, we therefore learn from Fig. 3(a) that at  $\omega_2$  ( $\omega_1$ ) the synchronous manifold falls on a periodic (chaotic) attractor. To check this, we plot in Figs. 3(b) and 3(c) the trajectories of the synchronous manifolds for  $\omega_2$  and  $\omega_1$ , respectively. Clearly, the trajectory is periodic for  $\omega_2$ , and is chaotic for  $\omega_1$ .

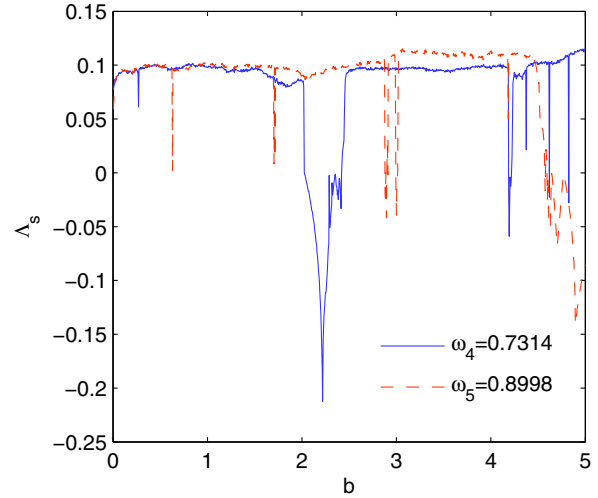


FIG. 4. (Color online) For  $\omega = 0.7134$  and  $0.8998$ , the variation of the largest Lyapunov exponent of the synchronous manifold,  $\Lambda_s$ , as a function of the driving amplitude.

So far we have fixed the driving amplitude to  $b = 4$ . One may wonder whether the sensitive dependence to frequency would also persist when varying the driving amplitude. In Fig. 4, we plot, for two arbitrarily chosen frequencies  $\omega = 0.7134$  and  $0.8998$ , the largest Lyapunov exponent of the synchronous manifold,  $\Lambda_s$ , as a function to the driving amplitude. One can see that, at certain values of driving amplitude (as the downward spikes indicate), the oscillator's motion changes abruptly from chaotic ( $\Lambda_s \sim 0.1$ ) to periodic ( $\Lambda_s \lesssim 0$ ). Therefore, the behavior of sensitive dependence relies on both the driving frequency and the driving amplitude. Although the frequency dependence can be originated from the intrinsic periodic orbits embedded in the chaotic motion, the amplitude dependence can be more subtle and deserves further investigation.

Combining the results of Figs. 2, 3, and 4, the phenomenon of synchronization sensitivity, as shown in Fig. 1, can now be understood as follows. First, due to the externally added periodic driving, the node dynamics is significantly modified. In particular, at some specific frequencies the node dynamics becomes periodic. The modified node dynamics in turn affects the MSF curve, reflecting as an adjustment of the boundaries of the stable region. As the network structure is fixed, by adjusting the boundaries of the stable region, the stability of the nontrivial eigenmodes will be changed. Generally speaking, the wider the stable region is, the higher the possibility will be for the nontrivial eigenmodes to become stable, and the higher the network synchronizability is. Comparing to the chaotic motion, the stable region of periodic motion is significantly enlarged. In particular, for periodic oscillators, the dynamics are synchronizable in the small coupling limit, i.e., the system of coupled identical periodic oscillators will synchronize for arbitrarily small coupling strength, although the time to arrive at synchronization can be long. While for the chaotic oscillator, the region for negative MSF can be highly case dependent, the common point is that for the small coupling limit, the system will not synchronize, which is guaranteed by the fact that the MSF is positive when the normalized coupling parameter  $\sigma$  is

zero. Therefore, whenever the nodal dynamics are perturbed from chaotic to periodic, the negative region of MSF will change abruptly from excluding the zero point to including the zero point. As such, at frequencies of periodic node motion the network synchronizability will be dramatically enhanced, e.g., the case of  $\omega_2$  shown in Fig. 1. Finally, according to previous studies of chaos control [31,32], periodic motion occurs when the frequency of the external force is resonant with the intrinsic frequencies of the chaotic motion. For the typical chaotic motion, the intrinsic frequencies are associated with the embedded unstable periodic orbits (UPO), which are densely distributed in the attractor. For this reason, the sensitivity of network synchronization is only observable at these resonant frequencies. This also explains why  $\sigma_1$  and  $\sigma_2$  are varying so wildly with  $\omega$  in Figs. 2(b) and 2(c). Note that the above arguments are for the case when the driving amplitude and the driving frequency are properly chosen that the dynamics for a single node have been significantly changed, as demonstrated in Fig. 3. If the external driving fails to modify the nodal dynamics in such an effective way, e.g., if the driving amplitude is too weak or the chaotic motion does not possess distinct frequencies, the above argument will be not applicable and the relationship deserves further investigation.

#### IV. GENERALIZATION

To check the generality of the observed phenomenon, we replace the Rössler oscillator with the Hindmarsh-Rose (HR) oscillator, and investigate the dependence of network synchronization on external driving again with the same ER random network. The HR oscillator describes the spiking-bursting behaviors of the neuron membrane potential, and has been widely used in literature for exploring various neuronal activities [33,34]. The HR oscillator is described by the equations

$$\begin{aligned} & (dx/dt, dy/dt, dz/dt)^T \\ & = [y + V(x) - z + I, 1 - 5x^2 - y, -rz + rs(x + 1.6)]^T, \end{aligned}$$

with  $V(x) = 3x^2 - x^3$ . By the parameters  $I = 3.2$ ,  $r = 6 \times 10^{-3}$ , and  $s = 4$ , the oscillator is of chaotic motion [33]. We adopt the coupling function  $\mathbf{H}([x, y, z]^T) = [y, 0, 0]^T$ , and add the periodic driving,  $g(t) = b \sin(\omega t)$ , on the  $y$  variable of each oscillator. The coupling strength is fixed at  $\varepsilon = 0.6$ , with which the network is not synchronized when the external driving is absent.

Like the Rössler oscillator, the MSF curve for the HR oscillator also has a bounded stable region. Specifically, we have  $\sigma_1 = 0.286$  and  $\sigma_2 = 1.233$  when the external driving is absent. This time, to capture the change of the stable region, we monitor the variation of the boundary ratio  $R_c = \sigma_2/\sigma_1$  as a function of the driving frequency  $\omega$ . The numerical results are presented in Fig. 5(a), where the driving amplitude is fixed as  $b = 0.5$ . It is seen that as  $\omega$  varies, the value of  $R_c$  is fluctuating with large amplitudes, especially for  $\omega \in [0, 0.285]$ . As  $R_c$  reflects the range of the stable region, the variation of  $R_c$  therefore implies the modified network synchronizability by varying the driving frequency. To show the sensitivity of the network synchronization further, we vary  $\omega$  adiabatically from zero to 0.285 (with the speed  $1 \times 10^{-9}$ ), and plot in Fig. 5(b) the time evolution of the network synchronization error  $\delta$ . It

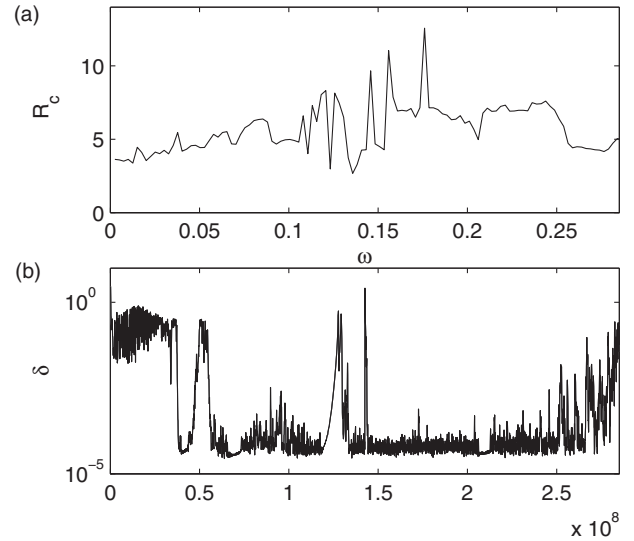


FIG. 5. For the model of networked chaotic HR oscillator, the dependence of network synchronization on the driving frequency,  $\omega$ . The amplitude of the driving is fixed as  $b = 0.5$ . (a) The variation of the boundary ratio  $R_c = \sigma_2/\sigma_1$  as a function of  $\omega$ . (b) By increasing  $\omega$  adiabatically from 0 to 0.285 (with the speed  $1 \times 10^{-9}$ , the time evolution of the network synchronization error,  $\delta$ .

is seen that as  $\omega$  increases, the network is transiting between the synchronous and nonsynchronous states in an intermittent fashion.

For autonomous systems like the Rössler and HR oscillators, the system dynamics is independent of the phase lag of the external driving,  $\phi_0$ . But for nonautonomous oscillators, e.g., the Duffing oscillator, as it has an intrinsic oscillation, the system dynamics could be dependent on the phase lag  $\phi_0$  between the intrinsic oscillation and the external driving [35,36]. This makes it possible to modify the synchronization of networked nonautonomous oscillators by changing the phase of the external driving. To justify this, we replace the node dynamics with the Duffing oscillator, and study the dependence of network synchronization on  $\phi_0$  with the same ER random network. The Duffing oscillator in its isolated form is described by the equations  $(dx/dt, dy/dt)^T = (y, -vy - x^3 + \beta \cos \omega' t)^T$ . For the parameters  $v = 0.3$ ,  $\beta = 8.85$ , and  $\omega' = 1$ , the oscillator is chaotic, with the largest Lyapunov exponent being about 0.1 [35]. The oscillators are coupled through the  $x$  variable, i.e.,  $\mathbf{H}([x, y]^T) = [x, 0]^T$ . For such coupled Duffing oscillators, the stable region of the MSF curve is open at the right side, i.e.,  $\Lambda(\sigma) < 0$  for  $\sigma > \sigma_1 \approx 0.22$  [26]. The coupling strength is chosen as  $\varepsilon = 0.012$ , with which the network is not synchronized when the external driving is absent. The external driving,  $g(t) = b \cos(\omega t + \phi_0)$ , is added on the  $y$  component of each oscillator. The amplitude and frequency of the driving are set as  $b = 0.66$  and  $\omega = 3\omega'$ , respectively.

We first check the influence of  $\phi_0$  on the stable region of the MSF curve. As now the stable region is open at the right side, we only need to monitor the left boundary,  $\sigma_1$ . By numerical simulations, we plot in Fig. 6 the variation of  $\sigma_1$  as a function of  $\phi_0$  for  $\phi_0 \in [0, 2\pi)$ . It is shown that, similar to the effect of the driving frequency on autonomous systems,

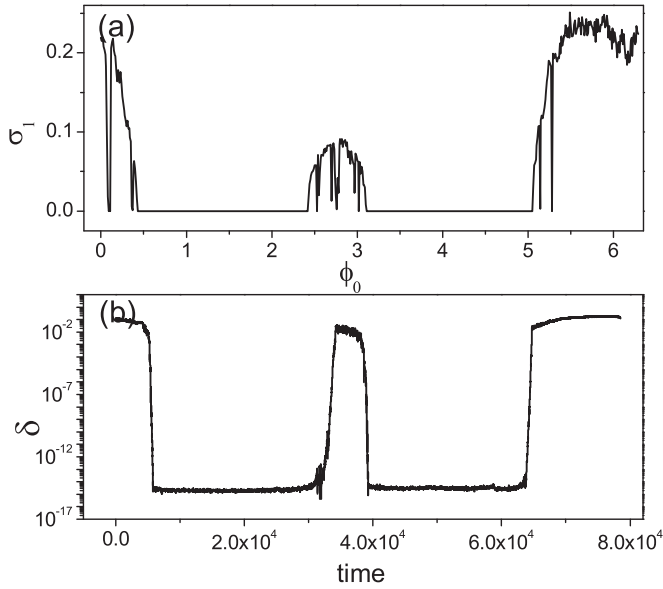


FIG. 6. For the model of networked chaotic Duffing oscillators, the dependence of network synchronization on the phase of the external driving. (a) The variation of  $\sigma_1$  as a function of the phase lag,  $\phi_0$ . (b) By the frequency mismatch  $\Delta\omega = 1 \times 10^{-3}$ , the evolution of the network synchronization error,  $\delta$ , as a function of time.

the stable region of the MSF curve is significantly modified by the phase lag of the driving. In a realistic situation, it is impossible to have exactly  $\omega = 3\omega'$  for the external driving. As such, there will be a small mismatch between the two frequencies,  $\Delta\omega = \omega - 3\omega'$ . This frequency mismatch will introduce a phase drifting,  $\Delta\omega t$ , which, according to Fig. 6(a), will make the network switch between the synchronous and nonsynchronous states in an automatic fashion. To demonstrate this interesting phenomenon, we set  $\Delta\omega = 8 \times 10^{-4}$ , and plot in Fig. 6(b) the time evolution of the network synchronization error,  $\delta$ . Indeed, it is shown that as time increases, the network is switching between the synchronous and nonsynchronous states automatically.

## V. DISCUSSIONS AND CONCLUSION

The effect of random perturbations has been also tested, where the network synchronization is found to be hardly affected. For instance, in the model of networked chaotic Rössler oscillators, if we replace the driving with the random perturbations,  $g(t) = [D\xi(t), 0, 0]^T$ , with  $\xi(t)$  a random variable of uniform probability distribution in  $[-1, 1]$  and  $D$  the noise amplitude, it is shown that the MSF curve is almost unchanged even for  $D = 10$ . Although previous studies have shown that under some circumstances chaos synchronization can be induced by common noise, the noise amplitude required there is usually very large, e.g.,  $D \approx 30$  for the chaotic Lorenz oscillator [37]. For the model of networked chaotic Rössler oscillators (with the parameters the same to Fig. 1), we have increased the noise amplitude up to  $D = 20$  (beyond which the oscillator is unstable), and found that the network is still not synchronized. Hence, comparing with the random perturbations, the periodic driving is much more effective in affecting the network synchronization.

The finding that network synchronization is sensitive to the frequency and phase of external driving might be useful for the purpose of synchronization control. Previously, the control of network synchronization is mainly achieved by pinning a portion of the network nodes to an externally added controller, i.e., the approach of pinning synchronization [38,39]. Comparing with pinning synchronization, the alternative approach is based on a different mechanism, and could be more efficient and feasible in certain circumstances. In pinning synchronization, the controller has the same dynamics and coupling function as the network nodes, which makes the relevant studies essentially a problem of network synchronization, and therefore can be treated under the framework of MSF analysis. In fact, in pinning synchronization the role of the controller is to introduce a *super* node (of a large number of connections) to the existing network, which modifies the eigenvalues of the network coupling matrix and, in turn, changes the network synchronizability. Different from that, in our alternative approach the network eigenvalues are fixed, and the control of network synchronization is achieved by modifying the MSF curve. The interesting thing is that, by a slight change of the frequency or the phase lag of the external driving, the MSF curve could be dramatically changed in such a way that all the unstable modes are contained in the stable region. This feature makes the alternative approach more efficient than the pinning approach (in pinning control the unstable modes are shifted into the stable region progressively as the number of pinned nodes, or the pinning strength, increases). Moreover, as an open-loop control strategy, the alternative approach does not require *a priori* knowledge of the network structure; neither needs to know the instant states of the network nodes. This makes the alternative control approach more feasible in realistic applications.

In summary, we have studied the synchronization of networked chaotic oscillators when an external periodic driving is presented, and found that by a slight change of the frequency or phase of the driving, the network can be easily transited between the synchronous and nonsynchronous states. We have demonstrated this phenomenon by different models, and analyzed its underlying mechanism based on the MSF method. Notably, it is found that the modified network synchronization is rooted in the change of the MSF curve, instead of the network eigenvalues as widely adopted in the existing studies. Our studies highlight the importance of external driving in affecting the network synchronization, and also provide an alternative approach for controlling the synchronization behaviors in complex systems.

## ACKNOWLEDGMENTS

We thank Professor Ying-Cheng Lai, Professor Wenxu Wang, and Professor Louis Pecora for helpful discussions. This work was supported by the National Natural Science Foundation of China under Grants No. 11375109, No. 11135001, No. 11375074, and No. 11422541, and by the Fundamental Research Funds for the Central Universities under Grants No. GK201303002 and No. lzujbky-2014-33. W.Y. was also supported by China Scholarship Council under Grant No. 201406180073.

- [1] L. Gammaitoni, P. Hänggi, P. Jung, and F. Marchesoni, *Rev. Mod. Phys.* **70**, 223 (1998).
- [2] H. G. Schuster, *Handbook of Chaos Control* (Wiley-VCH, Weinheim, 1999).
- [3] W. L. Koukkari and R. B. Sothorn, *Introducing Biological Rhythms* (Springer, New York, 2006).
- [4] L. Glass and M. C. Mackey, *From Clocks to Chaos: The Rhythms of Life* (Princeton University Press, Princeton, NJ, 1988).
- [5] H. Irisawa, H. F. Brown, and W. Giles, *Physiol. Rev.* **73**, 197 (1993).
- [6] P. A. Merolla *et al.*, *Science* **345**, 668 (2014).
- [7] T. M. Antonsen, Jr., R. T. Faghih, M. Girvan, E. Ott, and J. Platis, *Chaos* **18**, 037112 (2008).
- [8] H. Kori and A. S. Mikhailov, *Phys. Rev. Lett.* **93**, 254101 (2004).
- [9] S. Luther *et al.*, *Nature (London)* **475**, 235 (2011).
- [10] X. Feng, X. Gao, D.-B. Pan, B.-W. Li, and H. Zhang, *Sci. Rep.* **4**, 4831 (2014).
- [11] M. Perc, *Phys. Rev. E* **76**, 066203 (2007).
- [12] Z. Liu, *Europhys. Lett.* **100**, 60002 (2012).
- [13] A. S. Pikovsky, M. G. Rosenblum, and J. Kurths, *Synchronization: A Universal Concept in Nonlinear Science* (Cambridge University Press, Cambridge, UK, 2001).
- [14] A. Arenas, A. Diaz-Guilera, J. Kurths, Y. Moreno, and C. S. Zhou, *Phys. Rep.* **469**, 93 (2008).
- [15] A. L. Barabási and R. Albert, *Science* **286**, 509 (1999).
- [16] D. J. Watts and S. H. Strogatz, *Nature (London)* **393**, 440 (1998).
- [17] X. F. Wang and G. Chen, *Int. J. Bifurcat. Chaos Appl. Sci. Eng.* **12**, 187 (2002).
- [18] T. Nishikawa, A. E. Motter, Y.-C. Lai, and F. C. Hoppensteadt, *Phys. Rev. Lett.* **91**, 014101 (2003).
- [19] M. Chavez, D.-U. Hwang, A. Amann, H. G. E. Hentschel, and S. Boccaletti, *Phys. Rev. Lett.* **94**, 218701 (2005).
- [20] A. E. Motter, C. S. Zhou, and J. Kurths, *Europhys. Lett.* **69**, 334 (2005).
- [21] X. Wang, Y.-C. Lai, and C.-H. Lai, *Phys. Rev. E* **75**, 056205 (2007); X. Wang, L. Huang, Y.-C. Lai, and C. H. Lai, *ibid.* **76**, 056113 (2007); L. Huang, Y.-C. Lai, K. Park, X. Wang, C. H. Lai, and R. A. Gatenby, *Front. Phys. China* **2**, 446 (2007); X. Wang, L. Huang, S.-G. Guan, Y.-C. Lai, and C. H. Lai, *Chaos* **18**, 037117 (2008).
- [22] L. Huang, K. Park, Y.-C. Lai, L. Yang, and K. Yang, *Phys. Rev. Lett.* **97**, 164101 (2006); L. Huang, Y.-C. Lai, and R. A. Gatenby, *Chaos* **18**, 013101 (2008); *Phys. Rev. E* **77**, 016103 (2008).
- [23] L. M. Pecora and T. L. Carroll, *Phys. Rev. Lett.* **80**, 2109 (1998).
- [24] G. Hu, J. Z. Yang, and W. Liu, *Phys. Rev. E* **58**, 4440 (1998).
- [25] M. Barahona and L. M. Pecora, *Phys. Rev. Lett.* **89**, 054101 (2002).
- [26] L. Huang, Q. Chen, Y.-C. Lai, and L. M. Pecora, *Phys. Rev. E* **80**, 036204 (2009).
- [27] M. J. Bünner and W. Just, *Phys. Rev. E* **58**, R4072(R) (1998); M. Zhan, X. Wang, X. Gong, G. W. Wei, and C.-H. Lai, *ibid.* **68**, 036208 (2003).
- [28] O. E. RöSSLer, *Phys. Lett. A* **57**, 397 (1976).
- [29] L. Donetti, P. I. Hurtado, and M. A. Muñoz, *Phys. Rev. Lett.* **95**, 188701 (2005).
- [30] C. Zhou, A. E. Motter, and J. Kurths, *Phys. Rev. Lett.* **96**, 034101 (2006).
- [31] T. Kapitaniak, *Controlling Chaos: Theoretical and Practical Methods in Nonlinear Dynamics* (Academic Press, London, 1996).
- [32] H. G. Schuster, *Handbook of Chaos Control* (Wiley-VCH, Weinheim, 1999).
- [33] J. L. Hindmarsh and R. M. Rose, *Proc. R. Soc. Lond. B* **221**, 87 (1984).
- [34] M. Dhamala, V. K. Jirsa, and M. Ding, *Phys. Rev. Lett.* **92**, 028101 (2004).
- [35] Z. Qu, G. Hu, G. Yang, and G. Qin, *Phys. Rev. Lett.* **74**, 1736 (1995).
- [36] X. Wang, Y.-C. Lai, and C. H. Lai, *Chaos* **16**, 023127 (2006).
- [37] A. Maritan and J. R. Banavar, *Phys. Rev. Lett.* **72**, 1451 (1994).
- [38] H. Gang and Q. Zhilin, *Phys. Rev. Lett.* **72**, 68 (1994).
- [39] L. Yang, X. G. Wang, Y. Li, and Z. Sheng, *Europhys. Lett.* **92**, 48002 (2010).